4202 *J. Phys. Chem. A* **1999,** *103,* 4202−4208

Atmospheric Degradation Mechanism of CF_3OCH_3

L. K. Christensen

Atmospheric Chemistry, Plant Biology and Biogeochemistry Department, Risø National Laboratory, DK-4000 Roskilde, Denmark

T. J. Wallington,*,[1] A. Guschin, and M. D. Hurley

Ford Research Laboratory, SRL-3083, Ford Motor Company, P.O. Box 2053, Dearborn, Michigan 48121-2053

Received: November 17, 1998; In Final Form: March 10, 1999

A smog chamber/FTIR technique was used to study the Cl atom initiated oxidation of CF_3OCH_3 in 700 Torr of N_2/O_2 at 296 K. Using relative rate techniques it was determined that $k(Cl + CF_3OCH_3) = (1.4 \pm 0.2) \times 10^{-13}$ and $k(Cl + CF_3OC(O)H) = (9.8 \pm 1.2) \times 10^{-15}$ cm^3 molecule^{-1} s^{-1}. At 700 Torr of N_2/O_2 diluent at 296 K reaction with O_2 is the only loss mechanism of the $CF_3OCH_2O^\bullet$ radical. The infrared spectra of the peroxy nitrates $CF_3OCH_2O_2NO_2$ and $CF_3OC(O)O_2NO_2$ were recorded and compared to the nonfluorinated analogues $CH_3OCH_2O_2NO_2$ and $CH_3OC(O)O_2NO_2$. The thermal decomposition rate of $CF_3OC(O)O_2NO_2$ is $(2.3 \pm 0.1) \times 10^{-4}$ s^{-1} in 700 Torr of N_2 at 295.8 K. The reaction of $CF_3OC(O)O_2$ radicals with HO_2 radicals gives $CF_3OC(O)H$ in a yield of (80 ± 11)%. The results are discussed with respect to the atmospheric degradation mechanism of CF_3OCH_3 and other ethers.

1. Introduction

Recognition of the adverse effect of chlorofluorocarbon (CFC) release into the atmosphere[2,3] has led to an international effort to replace CFCs with environmentally acceptable alternatives. Hydrofluoroethers (HFEs) are a class of compounds which have been developed to replace CFCs in applications such as the cleaning of electronic equipment, heat transfer agents in refrigeration systems, and carrier fluids for lubricant deposition.[4] HFEs are volatile compounds and are released into the atmosphere when used. CF_3OCH_3 has not been used commercially but is one of the simplest fluoroethers and serves as a model compound for the group of fluorinated ethers. The atmospheric oxidation of CF_3OCH_3 is initiated by reaction with OH radicals.

$$OH + CF_3OCH_3 \rightarrow CF_3OCH_2^\bullet + H_2O \qquad (1)$$

The kinetics of the reaction of OH with CF_3OCH_3 has been the subject of three investigations,[5−7] but the atmospheric degradation mechanism of CF_3OCH_3 has yet to be studied.

Under atmospheric conditions alkyl radicals produced in reaction 1 react with oxygen to give peroxy radicals.

$$CF_3OCH_2^\bullet + O_2 \rightarrow CF_3OCH_2O_2^\bullet \qquad (2)$$

By analogy to other peroxy radicals,[8] $CF_3OCH_2O_2^\bullet$ radicals will react with NO, NO_2, HO_2, and other peroxy radicals in the atmosphere.

$$CF_3OCH_2O_2^\bullet + NO \rightarrow CF_3OCH_2O^\bullet + NO_2 \qquad (3a)$$

$$CF_3OCH_2O_2^\bullet + NO + M \rightarrow CF_3OCH_2ONO_2 + M \qquad (3b)$$

$$CF_3OCH_2O_2^\bullet + NO_2 + M \rightleftarrows CF_3OCH_2O_2NO_2 + M \qquad (4)$$

$$CF_3OCH_2O_2^\bullet + HO_2 \rightarrow \text{products} \qquad (5)$$

$$CF_3OCH_2O_2^\bullet + R'O_2 \rightarrow \text{products} \qquad (6)$$

In this work the products of reactions 3 and 5, atmospheric fate of $CF_3OCH_2O^\bullet$ radicals, thermal stability of the peroxynitrate $CF_3OC(O)O_2NO_2$, and IR spectra of $CF_3OCH_2O_2NO_2$, $CF_3OC(O)O_2NO_2$, and the analogous nonfluorinated peroxynitrates $CH_3OCH_2O_2NO_2$, $CH_3OC(O)O_2NO_2$, and $HC(O)OCH_2O_2NO_2$ have been studied.

2. Experimental Section

FTIR Smog Chamber Setup. All experiments were performed in a 140-L Pyrex reactor interfaced to a Mattson Sirus 100 FTIR spectrometer.[9] The optical path length of the infrared beam was 27 m. The reactor was surrounded by 22 fluorescent blacklamps (GE F15T8-BL) which were used to photochemically initiate the experiments. The oxidation of CF_3OCH_3 was initiated by reaction with Cl atoms which were generated by the photolysis of molecular chlorine in 700 Torr total pressure of O_2/N_2 diluent at 295 ± 2 K,

$$Cl_2 + h\nu \rightarrow 2Cl$$

$$Cl + CF_3OCH_3 \rightarrow CF_3OCH_2^\bullet + HCl \qquad (7)$$

$$CF_3OCH_2^\bullet + O_2 + M \rightarrow CF_3OCH_2O_2^\bullet + M \qquad (2)$$

Loss of CF_3OCH_3 and the formation of products were measured

---

* To whom correspondence should be addressed.

10.1021/jp984455a CCC: $18.00 © 1999 American Chemical Society
Published on Web 05/06/1999

by FTIR spectroscopy at a resolution of 0.25 cm^{-1}. IR spectra were derived from 32 coadded interferograms.

The CF_3OCH_3 sample was provided by Vladimir Orkin (National Institute of Standards and Technology). FTIR analysis revealed the presence of 3% CH_3F impurity and an unidentified impurity with an absorption feature at 712 cm^{-1}. To obtain a calibrated spectrum of CF_3OCH_3 a pure CF_3OCH_3 sample was achieved by freeze−pump−thaw cycling which removed all traces of CH_3F and the unknown.

In smog chamber experiments unwanted loss of reactants and products via photolysis, dark chemistry, and wall reactions have to be considered. Control experiments were performed to check for such unwanted losses of CF_3OCH_3 in the chamber; none were observed. No loss of $CF_3OC(O)H$ was observed when reaction mixtures containing $CF_3OC(O)H$ and Cl_2 were left to stand in the dark showing that dark chemistry and heterogeneous loss of $CF_3OC(O)H$ in the chamber are not important. By analogy to the nonfluorinated analogue $CH_3OC(O)H$ which does not absorb at wavelengths greater than 260 nm,[10] it seems highly unlikely that photolysis of $CF_3OC(O)H$ will be significant in the chamber.

Four sets of experiments were performed. First, relative rate techniques were used to determine rate constants for the reactions of Cl atoms with CF_3OCH_3 and $CF_3OC(O)H$. Second, the products of the atmospheric oxidation of CF_3OCH_3 in the presence of NO_x were determined. Third, the mechanism of the reaction of $CF_3OCH_2O_2^{\bullet}$ with HO_2 radicals was studied. Fourth, the IR spectra and thermal stability of the peroxy nitrates $CF_3OCH_2O_2NO_2$ and $CF_3OC(O)O_2NO_2$ were investigated.

3. Results

3.1. Relative Rate Measurement of $k(Cl + CF_3OCH_3)$. The kinetics of reaction 7 were measured relative to reactions 8 and 9.

$$Cl + CF_3OCH_3 \rightarrow CF_3OCH_2^{\bullet} + HCl \quad (7)$$

$$CH_3Cl + Cl \rightarrow \text{products} \quad (8)$$

$$CH_4 + Cl \rightarrow \text{products} \quad (9)$$

The initial concentrations were 6.5−7.5 mTorr of CF_3OCH_3, 150−260 mTorr of Cl_2, and 12−16 mTorr of either CH_4 or CH_3Cl in 700 Torr of either air or N_2 diluent. The observed loss of CF_3OCH_3 versus those of reference compounds in the presence of Cl atoms is shown in Figure 1. Absorption bands used for spectral subtraction were at 1171 and 1298 cm^{-1} for CF_3OCH_3, 739 cm^{-1} for CH_3Cl, and 1306 cm^{-1} for CH_4. Linear least-squares analysis of the data in Figure 1 gives $k_7/k_8 = 0.284 \pm 0.014$ and $k_7/k_9 = 1.36 \pm 0.10$. Using $k_8 = 4.8 \times 10^{-13}$ and $k_9 = 1.0 \times 10^{-13}$ cm^3 $molecule^{-1}$ s^{-1},[11] we derive $k_7 = (1.36 \pm 0.07) \times 10^{-13}$ and $(1.36 \pm 0.10) \times 10^{-13}$ cm^3 $molecule^{-1}$ s^{-1}. We estimate that potential systematic errors associated with uncertainties in the reference rate constants add 10% uncertainty range for k_7. Propagating this additional uncertainty gives $k_7 = (1.36 \pm 0.15) \times 10^{-13}$ and $(1.36 \pm 0.17) \times 10^{-13}$ cm^3 $molecule^{-1}$ s^{-1}. We choose to cite a final value for k_7 which is the average of those determined using the two different reference compounds together with error limits which encompass the extremes of the individual determinations. Hence, $k_7 = (1.4 \pm 0.2) \times 10^{-13}$ cm^3 $molecule^{-1}$ s^{-1}. Quoted error reflects the accuracy of the measurements.

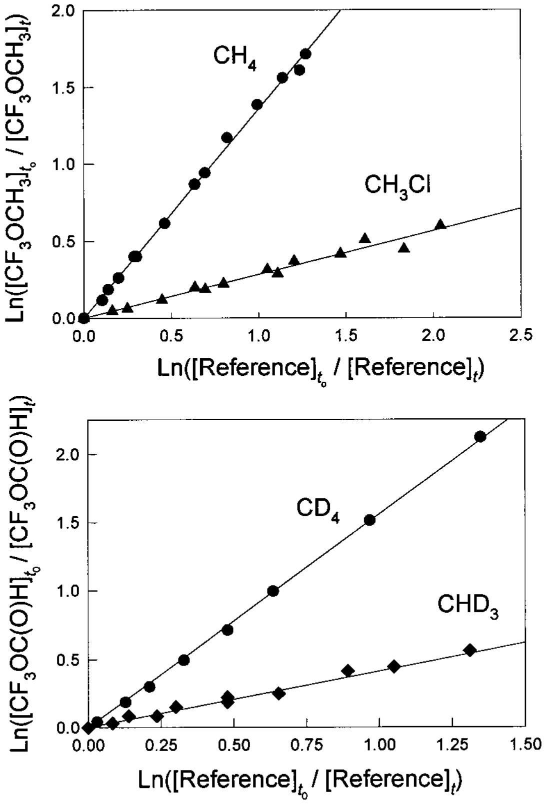

Figure 1. Top: Loss of CF_3OCH_3 versus loss of CH_4 (circles) and CH_3Cl (triangles) in the presence of Cl atoms in 700 Torr of either air or N_2 diluent. Bottom: Loss of $CF_3OC(O)H$ versus CD_4 (circles) and CHD_3 (diamonds) in the presence of Cl atoms in 700 Torr of air.

3.2. Relative Rate Measurement of $k(Cl + CF_3OC(O)H)$. As discussed in section 3.3, trifluoromethyl formate was readily generated in the chamber by UV irradiation of gas mixtures of 4−13 mTorr of CF_3OCH_3 and 0.4−0.7 Torr of Cl_2 in 700 Torr of air. After all (more than 97%) of CF_3OCH_3 was converted into $CF_3OC(O)H$ a reference compound (CD_4 or CHD_3) was added and the UV irradiation was resumed.

$$CF_3OC(O)H + Cl \rightarrow CF_3OC(O)^{\bullet} + HCl \quad (10)$$

$$CD_4 + Cl \rightarrow \text{products} \quad (11)$$

$$CHD_3 + Cl \rightarrow \text{products} \quad (12)$$

The rate constant k_{10} was derived by observing the relative loss rates of $CF_3OC(O)H$ and the reference compounds. Absorption bands used for spectral subtraction were 1107 and 1807 cm^{-1} for $CF_3OC(O)H$, 996 cm^{-1} for CD_4, and 1036 cm^{-1} for CHD_3. The results are shown in Figure 1.

Linear least-squares analysis of the data in Figure 1 gives $k_{10}/k_{11} = 1.59 \pm 0.02$ and $k_{10}/k_{12} = 0.43 \pm 0.02$. Using $k_{11} = 6.1 \times 10^{-15}$ and $k_{12} = 2.32 \times 10^{-14}$ cm^3 $molecule^{-1}$ s^{-1},[12] we derive $k_{10} = (9.7 \pm 0.1) \times 10^{-15}$ and $(10.0 \pm 0.5) \times 10^{-15}$ cm^3 $molecule^{-1}$ s^{-1}. We estimate that potential systematic errors associated with uncertainties in the reference rate constants add an 10% uncertainty range for k_{10}. Propagating this additional uncertainty gives $(9.7 \pm 1.0) \times 10^{-15}$ and $(10 \pm 1) \times 10^{-15}$ cm^3 $molecule^{-1}$ s^{-1}. We choose to cite a final value for k_{10} which is the average of those determined using the two different reference compounds together with error limits which encompass the extremes of the individual determinations. Hence, $k_{10} = (9.8 \pm 1.2) \times 10^{-15}$ cm^3 $molecule^{-1}$ s^{-1}. Quoted error reflects the accuracy of the measurements. The rate constant k_{10} is 14 times lower than k_7. This is consistent with the behavior of other formates, which are typically significantly less reactive toward Cl atoms than the ethers from which they are derived; for

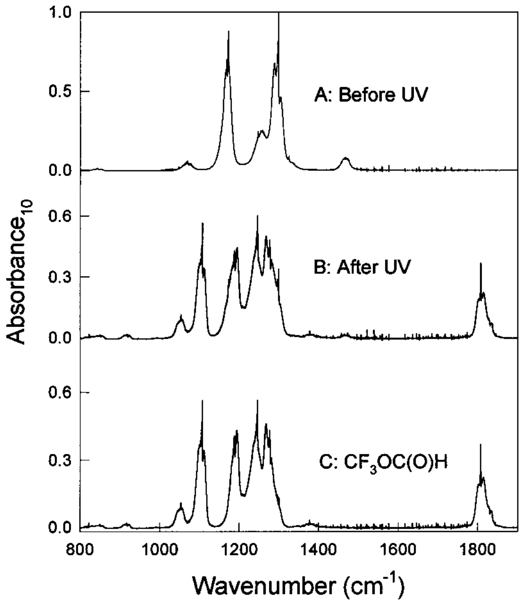

Figure 2. Infrared spectra acquired before (A) and after (B) 1 min irradiation of a mixture of 7.5 mTorr of CF_3OCH_3 and 275 mTorr of Cl_2 in 700 Torr of air. Panel C shows the product spectrum obtained after subtracting features attributable to CF_3OCH_3 from panel B.

example, $k(Cl + CH_3OCH_3)/k(Cl + CH_3OC(O)H) = 130$ [13,14] and $k(Cl + C_4F_9OCH_3)/k(Cl + C_4F_9OC(O)H) = 5$.[15]

3.3. Atmospheric Fate of $CF_3OCH_2O^\bullet$ Radicals. To investigate the atmospheric fate of $CF_3OCH_2O^\bullet$ radicals experiments were performed using the UV irradiation of $CF_3OCH_3/Cl_2/O_2/N_2$ mixtures with, and without, added NO. During the UV irradiation, peroxy radicals are formed by reactions 7 and 2. In the absence of NO, $CF_3OCH_2O^\bullet$ radicals are formed by the peroxy radical self-reaction (eq 6a).

$$2CF_3OCH_2O_2^\bullet \rightarrow 2CF_3OCH_2O^\bullet + O_2 \qquad (6a)$$

$$2CF_3OCH_2O_2^\bullet \rightarrow CF_3OC(O)H + CF_3OCH_2OH + O_2 \qquad (6b)$$

In the presence of NO, $CF_3OCH_2O^\bullet$ radicals are formed by reaction 3a.

$$CF_3OCH_2O_2^\bullet + NO \rightarrow CF_3OCH_2O^\bullet + NO_2 \qquad (3a)$$

$$CF_3OCH_2O_2^\bullet + NO \rightarrow CF_3OCH_2ONO_2 \qquad (3b)$$

Once formed, the $CF_3OCH_2O^\bullet$ radicals are expected to either react with oxygen to form trifluoromethyl formate or decompose to give $CF_3O^\bullet$ radicals and HCHO.

$$CF_3OCH_2O^\bullet + O_2 \rightarrow CF_3OC(O)H + HO_2 \qquad (13)$$

$$CF_3OCH_2O^\bullet + M \rightarrow CF_3O^\bullet + HCHO \qquad (14)$$

$CF_3O^\bullet$ radicals react rapidly with NO to give COF_2.[16]

$$CF_3O^\bullet + NO \rightarrow FNO + COF_2 \qquad (15)$$

The formation of $CF_3OC(O)H$ provides a marker for the importance of reaction 13 while formation of COF_2 serves as a marker for reaction 14. COF_2 is stable in the chamber and can be easily detected by its characteristic IR absorption in the 770–780 and 1850–2000 cm^{-1} regions.

Figure 2 shows spectra acquired before (A) and after (B) a 1 min irradiation of a mixture of 7.5 mTorr of CF_3OCH_3, 275 mTorr of Cl_2, in 700 Torr of air diluent. Subtraction of IR features attributable to CF_3OCH_3 from panel B gives the product spectrum shown in panel C. There was no evidence for the formation of COF_2 (less than 2%) in experiments (both with and without added NO) showing that decomposition via reaction 14 is not a significant fate of $CF_3OCH_2O^\bullet$ radicals. The IR spectrum of the product(s) shown in Figure 2C matches that calculated for $CF_3OC(O)H$.[15] Interestingly, all of the observed IR bands in the product spectrum shown in Figure 2C can be attributed to $CF_3OC(O)H$; the assignments are listed in Table 1. The concentration of the product observed following the UV irradiation of $CF_3OCH_3/Cl_2/O_2/N_2$ and $CF_3OCH_3/Cl_2/O_2/N_2/NO$ gas mixtures increased linearly with the consumption of CF_3OCH_3 over the range of consumption studied (5–80%).

TABLE 1: Comparison of Calculated[15] and Measured Frequencies (cm^{-1}) for the IR Spectrum of $CF_3OC(O)H$, Numbers in Parentheses are Relative Intensities

	syn-$CF_3OC(O)H$		*anti*-$CF_3OC(O)H$	
	calcd	measd	calcd	measd
$\nu(C_H{=}O)$	1800 (55)	1807	1823 (13)	1834
$\nu(H-C_H-O)$	1351 (3)	1377	1377 (1)	
$\nu(F-C_F)$	1284 (66)	1277	1309 (23)	
$\nu(F-C_F)$	1260 (62)	1246	1250 (22)	
$\nu(C_F-O)$	1199 (100)	1187	1224 (16)	
$\nu(C_O-O)$	1129 (32)	1107	1086 (9)	

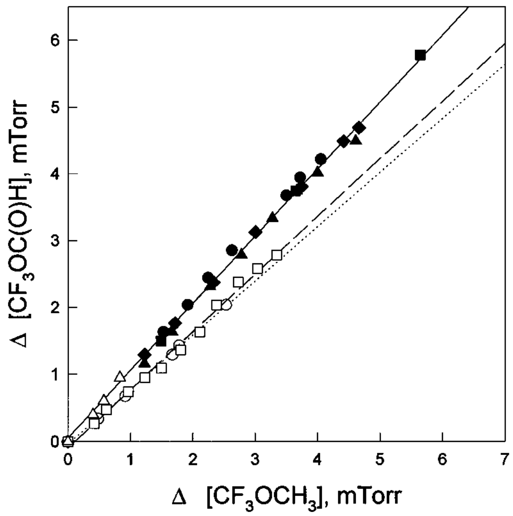

Figure 3. Formation of $CF_3OC(O)H$ versus loss of CF_3OCH_3 at a total pressure of 700 Torr in mixtures of 5 mTorr CF_3OCH_3, 0.3 Torr Cl_2, and 6 Torr O_2 (filled triangles), 5 mTorr CF_3OCH_3, 0.6 Torr Cl_2, and 147 Torr O_2 (filled circles), 8 mTorr CF_3OCH_3, 0.3 Torr Cl_2, and 147 Torr O_2 (filled squares), 5 mTorr CF_3OCH_3, 0.3 Torr Cl_2, and 700 Torr O_2 (filled diamonds), 4.4 mTorr CF_3OCH_3, 0.07 Torr Cl_2, 0.7 Torr H_2, and 147 Torr O_2 (open circles), 5 mTorr CF_3OCH_3, 0.5 Torr Cl_2, 14 mTorr NO, and 127 Torr O_2 (open squares), and 6.37 mTorr CF_3OCH_3, 0.3 Torr Cl_2, 4.44 mTorr NO, and 130 Torr O_2 (open triangles).

In light of the fact that all of the product features in experiments conducted in the absence of NO can be assigned to $CF_3OC(O)H$, it seems reasonable to assume that CF_3OCH_3 is converted into $CF_3OC(O)H$ in essentially a 100% yield in such experiments. This assumption is the basis of the *y*-axis scale in Figure 3. It is possible that CF_3OCH_2OH could form in the peroxy radical self-reaction. No absorption features was observed that could be ascribed to an alcohol. Alcohols are generally very reactive toward Cl atoms, e.g., $k(Cl + CH_3OH) = 5 \times 10^{-11}$, $k(Cl + CH_2ClCH_2OH) = 3 \times 10^{-11}$ cm^3 molecule^{-1} s^{-1}, $k(Cl + n\text{-}C_4H_9OH) = 2 \times 10^{-10}$, and $k(Cl + ClCH_2OH) = 4 \times 10^{-12}$ cm^3 molecule^{-1} s^{-1}.[17] If CF_3OCH_2OH is formed in a significant yield, it would probably react with Cl atoms in the chamber and be converted to $CF_3OC(O)H$ by a mechanism analogous to the formation of formaldehyde from methanol.

Two experiments were performed in the presence of NO_x using mixtures of 5−6.4 mTorr of CF_3OCH_3, 130 Torr of O_2, 0.3−0.5 mTorr of Cl_2, and 4.4−14 mTorr of NO in 700 Torr total pressure with N_2. When NO is present in the reaction mixtures, the alkoxy radicals are formed via reaction 3a rather than reaction 6a. For experiments using the lowest NO concentration (and for 7−14% conversion of CF_3OCH_3) the observed yields of $CF_3OC(O)H$ were, within the experimental uncertainties, indistinguishable from that observed in the absence of NO (open triangles in Figure 3). It has previously been reported[18,19] that the reactions of NO with $CF_3CFHO_2^\bullet$ and $CF_3CF_2CFHO_2^\bullet$ radicals form chemically activated alkoxy radicals, which are more likely to decompose via C−C bond scission than alkoxy radicals formed by the $CF_3CFHO_2^\bullet$ and $CF_3CF_2CFHO_2^\bullet$ self-reactions. The results presented here show that the fate of the $CF_3OCH_2O^\bullet$ radicals is not dependent upon their source. For experiments using NO concentrations of 14 mTorr the observed yields of $CF_3OC(O)H$ were slightly (14%) lower than that observed in experiments conducted in the absence of NO (open squares in Figure 3). Additional IR product features at 760, 1011, 1231, 1284, and 1347 cm^{-1} attributable to one or more unknown product(s) were observed in experiments conducted in the presence of NO_x. These features are not attributable to the peroxy nitrate $CF_3OCH_2O_2NO_2$ (see section 3.5) but may be attributable to the nitrite CF_3OCH_2ONO or the nitrate $CF_3OCH_2ONO_2$ (or both) formed via association reaction of the alkoxy radical with NO or NO_2.

As shown with filled symbols in Figure 3, variation of the O_2 partial pressure over the range 6−700 Torr had no discernible impact on the yield of $CF_3OC(O)H$. We conclude that reaction 13 is the sole atmospheric fate of $CF_3OCH_2O^\bullet$ radicals. The behavior of $CF_3OCH_2O^\bullet$ radicals is consistent with those of the structurally similar alkoxy radicals i-$C_4F_9OCH_2O^\bullet$,[15] $CH_3OCH_2O^\bullet$,[13] and $(CH_3)_3COCH_2O^\bullet$ [20] which also undergo reaction with O_2 to give the corresponding formates.

For Cl atom initiated oxidation experiments conducted in the absence of NO we usually observe the formation of hydroperoxides via the reaction $RO_2 + HO_2 \rightarrow ROOH + O_2$ ($R = CF_3OCH_2$). The absence of hydroperoxides in the present experiments can be rationalized in several ways: (i) The $RO_2 + HO_2$ reaction is unusually slow. (ii) The $RO_2 + HO_2$ reaction does not give ROOH but instead produces the formate (the analogous $CH_3OCH_2O_2^\bullet + HO_2$ reaction gives a substantial formate yield[14]). (iii) ROOH is formed in the system but is consumed by secondary reaction with Cl atoms to regenerate the peroxy radical. (iv) There is a combination of i-iii. As discussed in the following section, the most likely explanation of the absence of ROOH is that the $RO_2 + HO_2$ reaction gives a substantial yield of the formate.

3.4. Mechanism of the $CF_3OCH_2O_2 + HO_2$ Reaction. To investigate the mechanism of reaction 5 a mixture of 4.4 mTorr of CF_3OCH_3, 74 mTorr of Cl_2, and 740 mTorr of H_2 in 700 Torr of air was introduced into the reaction chamber and irradiated using the UV fluorescent lamps. The chlorine atoms react with CF_3OCH_3 and H_2 to give CF_3OCH_2 radicals and H atoms

$$Cl + CF_3OCH_3 \rightarrow HCl + CF_3OCH_2^\bullet \tag{7}$$

$$Cl + H_2 \rightarrow HCl + H \tag{16}$$

which then add O_2 to give $CF_3OCH_2O_2^\bullet$ and HO_2 radicals. The relative flux of HO_2 and $CF_3OCH_2O_2^\bullet$ radicals is given by

$$\frac{d[HO_2]/dt}{d[CF_3OCH_2O_2^\bullet]/dt} = \frac{k_{16}}{k_7}\frac{[H_2]}{[CF_3OCH_3]}$$

For the given concentrations and $k_{16} = 1.6 \times 10^{-14}$ cm^3 $molecule^{-1}$ s^{-1},[11] HO_2 radicals are formed 19 times faster than $CF_3OCH_2O_2^\bullet$. There are no data available on the rate constants of reactions 6 and 5, but it seems reasonable to assume that the rate constant ratio k_5/k_6 is similar to that of the analogous reactions of the $HOCH_2O_2$ radical. The rate constant of the reaction of HO_2 with $HOCH_2O_2^\bullet$ is 1.3×10^{-11} cm^3 $molecule^{-1}$ s^{-1} while that of the $HOCH_2O_2^\bullet$ self-reaction is 6.2×10^{-12} cm^3 $molecule^{-1}$ s^{-1}.[21] For the experimental conditions used here it seems likely that reaction with HO_2 is essentially the sole fate of $CF_3OCH_2O_2^\bullet$ radicals.

The open circles in Figure 3 show the observed yield of $CF_3OC(O)H$ versus the loss of CF_3OCH_3 following the irradiation of the $CF_3OCH_3/H_2/Cl_2$/air mixture. Linear least-squares analysis gives a molar yield of $CF_3OC(O)H$ of 80 ± 11%. After subtraction of IR product features attributable to $CF_3OC(O)H$, residual IR features at 830 (very weak), 1034, and 1184 cm^{-1} were observed. Those residual features increased in intensity in proportion to the conversion of CF_3OCH_3. The IR feature at 830 cm^{-1} is typical for an O−O stretch, and we tentatively assign the residual spectrum to the hydroperoxide CF_3OCH_2OOH. From the observed yield of 80 ± 11% of $CF_3OC(O)H$, we conclude that $k_{5b}/(k_{5a} + k_{5b}) = 0.8$ and, by inference, $k_{5a}/(k_{5a} + k_{5b}) = 0.2$.

$$CF_3OCH_2O_2^\bullet + HO_2 \rightarrow CF_3OCH_2OOH + O_2 \tag{5a}$$

$$CF_3OCH_2O_2^\bullet + HO_2 \rightarrow CF_3OC(O)H + H_2O + O_2 \tag{5b}$$

This result is consistent with the available literature database concerning reaction of peroxy radicals with HO_2 in which the presence of electron-withdrawing groups such as F,[22] Cl,[23] and OCH_3[14] increase the importance of the carbonyl-forming reaction channel.

3.5. Infrared Spectra of $CF_3OCH_2O_2NO_2$, $CF_3OC(O)O_2NO_2$, $CH_3OCH_2O_2NO_2$, $CH_3OC(O)O_2NO_2$, and $HC(O)OCH_2O_2NO_2$. The peroxy nitrates $CF_3OCH_2O_2NO_2$ and $CH_3OCH_2O_2NO_2$ were prepared in the chamber by UV radiation of gas mixtures of (i) 8 mTorr of CF_3OCH_3, 0.3 Torr of Cl_2, 12 mTorr of NO_2 and (ii) 29 mTorr of CH_3OCH_3, 0.1 Torr of Cl_2, 22 mTorr of NO_2, respectively, in 700 Torr of O_2. The peroxy nitrates, $CX_3OCH_2O_2NO_2$, where X = F or H, are formed by the sequence of reactions

$$Cl + CX_3OCH_3 \rightarrow HCl + CX_3OCH_2^\bullet \tag{17}$$

$$CX_3OCH_2^\bullet + O_2 + M \rightarrow CX_3OCH_2O_2^\bullet + M \tag{18}$$

$$CX_3OCH_2O_2^\bullet + NO_2 + M \rightarrow CX_3OCH_2O_2NO_2 + M \tag{19}$$

$CF_3OCH_2O_2NO_2$ and $CH_3OCH_2O_2NO_2$ were found to be thermally unstable and decompose to regenerate NO_2 and a peroxy radical.

$$CX_3OCH_2O_2NO_2 + M \rightarrow CX_3OCH_2O_2^\bullet + NO_2 + M \tag{20}$$

$CF_3OCH_2O_2^\bullet$ and $CH_3OCH_2O_2^\bullet$ either react with NO_2 to re-

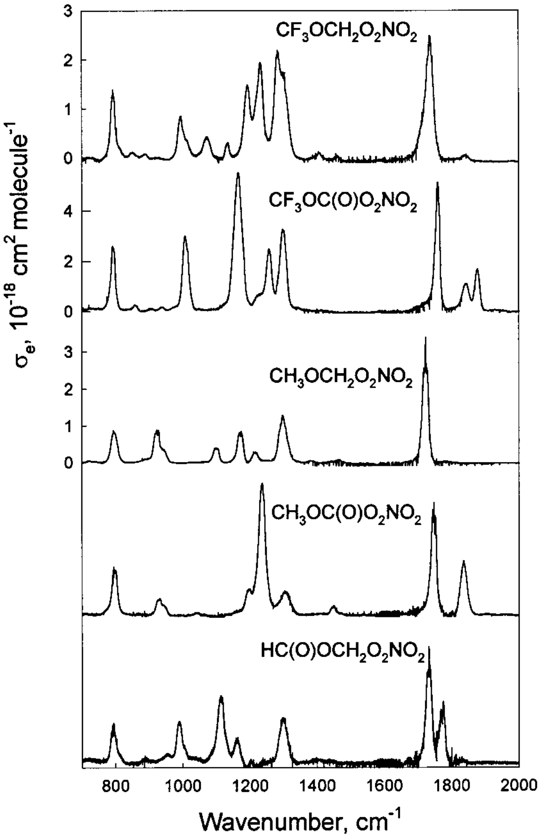

Figure 4. Infrared spectra of $CF_3OCH_2O_2NO_2$, $CF_3OC(O)O_2NO_2$, $CH_3OCH_2O_2NO_2$, $CH_3OC(O)O_2NO_2$, and $HC(O)OCH_2O_2NO_2$.

form the peroxy nitrate or undergo self-reaction to form the formate.

$$CX_3OCH_2O_2^{\bullet} + NO_2 + M \rightarrow CX_3OCH_2O_2NO_2 + M \quad (19)$$

$$2CX_3OCH_2O_2^{\bullet} \rightarrow 2CX_3OCH_2O^{\bullet} + O_2 \quad (21)$$

$$CX_3OCH_2O^{\bullet} + O_2 \rightarrow CX_3OCHO + HO_2 \quad (22)$$

By photolysis of mixtures containing Cl_2 and NO_x, compounds such as ClONO, $ClNO_2$, ClNO, and HNO_3 are formed. Infrared features from these products and from NO_2, $CF_3OC(O)H$, or $CH_3OC(O)H$ are subtracted from the measured spectra. The spectra of $CF_3OCH_2O_2NO_2$ and $CH_3OCH_2O_2NO_2$ are shown in Figure 4.

To record the IR spectrum of $CF_3OC(O)O_2NO_2$, trifluoromethyl formate was generated in the chamber by UV irradiation of gas mixtures of 18 mTorr of CF_3OCH_3 and 1 Torr of Cl_2 in 700 Torr of O_2. When CF_3OCH_3 was converted into $CF_3OC(O)H$, 12 mTorr of NO_2 was added and the UV irradiation was resumed. Using this procedure approximately 20% of $CF_3OC(O)H$ is lost via reaction 10 before NO_2 was added, and traces of CF_2O and CF_3OH were formed, together with a product that absorbs at 1170, 1256, and 1290 cm^{-1}. These absorption bands overlap with the $CF_3OC(O)O_2NO_2$ spectrum, and it was not possible to correct for the presence of this product. After 15 min of further UV irradiation 54% of trifluoromethyl formate was converted to $CF_3OC(O)O_2NO_2$, which was stable in the chamber (less than 2% loss in 25 min). Absorption features attributable to $CF_3OC(O)H$, HNO_3, NO_2, NO, $ClNO_2$ ClNO, ClONO, and N_2O_5 were subtracted from the final $CF_3OC(O)O_2NO_2$ spectrum shown in Figure 4.

To record the IR spectra of $CH_3OC(O)O_2NO_2$ and $HC(O)OCH_2O_2NO_2$, mixtures of 11−13 mTorr of $CH_3OC(O)H$, 13−19 mTorr of NO_2, and 160−170 mTorr of Cl_2 in 700 Torr of O_2 diluent were subject to UV irradiation. The reaction of Cl atoms with methyl formate proceeds via two channels:

$$Cl + CH_3OC(O)H \rightarrow CH_3OC(O)^{\bullet} + HCl \quad (23)$$

$$Cl + CH_3OC(O)H \rightarrow {}^{\bullet}CH_2OC(O)H + HCl \quad (24)$$

Product spectra obtained after $CH_3OC(O)H$ /NO_2/Cl_2/O_2 mixtures were subject to UV irradiation contain IR features attributable to both $CH_3OC(O)O_2NO_2$ and $HC(O)OCH_2O_2NO_2$. Acyl peroxy nitrates generally undergo thermal decomposition considerably more slowly than alkyl peroxy nitrates,[17] and it is reasonable to believe that $CH_3OC(O)O_2NO_2$ is more stable in the chamber than $HC(O)OCH_2O_2NO_2$. The spectra of the two peroxy nitrates can be separated by adding a small amount (4−5 mTorr in our experiments) of NO to the reaction mixture which causes a rapid loss of the less stable $HC(O)OCH_2O_2NO_2$ and formation of formic anhydride and formic acid. Reference spectra of pure HC(O)OC(O)H and HC(O)OH were used for spectral subtraction of these compounds. Spectra obtained using this approach are shown in Figure 4. Kirchner et al.[24] used a similar approach to generate $CH_3OC(O)O_2NO_2$, but unlike us they did not observe peroxy nitrate bands that rapidly disappeared when NO was added. The reason for this discrepancy is unknown. Nevertheless the absorption frequencies of $CH_3OC(O)O_2NO_2$ reported by Kirchner et al. are consistent with our observations. The major IR bands observed for the five peroxy nitrates are listed in Table 2.

The measured wavenumbers of NO_2 deformation, NO_2 symmetric and asymmetric stretches, and the C=O stretching modes for the five peroxy nitrates can be compared with the literature values for $CH_3C(O)O_2NO_2$.[25] For the six peroxy nitrates RO_2NO_2 with R = $CF_3OC(O)$, $CH_3OC(O)$, $CH_3C(O)$, CF_3OCH_2, CH_3OCH_2, or $HC(O)OCH_2$, the NO_2 deformation is always found between 791 and 797 cm^{-1}. It also appears that the nature of the substituent group R has very little influence on the position of the symmetric NO_2 stretch. The spectrum of $CF_3OCH_2O_2NO_2$ (Figure 4) shows two overlapping bands between 1283 and 1304 cm^{-1}, of which the weaker “right shoulder” at 1304 cm^{-1} is most likely the symmetric NO_2 stretch. The asymmetric NO_2 stretches are found at lower wavenumbers for alkyl peroxy nitrates than for acyl peroxy nitrates, i.e., 1723−1735 cm^{-1} for $CF_3OCH_2O_2NO_2$, $CH_3OCH_2O_2NO_2$, and $HC(O)OCH_2O_2NO_2$ and 1741−1759 cm^{-1} for $CF_3OC(O)O_2NO_2$, $CH_3OC(O)O_2NO_2$, and $CH_3C(O)O_2NO_2$. It is interesting that the spectrum of $CF_3OC(O)O_2NO_2$ shows two bands at 1843 and 1875 cm^{-1} in the carbonyl stretching region. This observation suggests that there are two stable conformers of $CF_3OC(O)O_2NO_2$, analogous to the syn- and anti-conformers of $CF_3OC(O)H$. The C=O stretch of $HC(O)OCH_2O_2NO_2$ is found at 1772 cm^{-1}, much lower than those of the acyl peroxy nitrates. The carbonyl stretch in $HC(O)OCH_2O_2NO_2$ can be compared with that of $HC(O)OCH_2OC(O)H$ (methylene glycol diformate).[26] The $HC(O)OCH_2OC(O)H$ spectrum has a strong isolated C=O stretch at 1769 cm^{-1}, which is in very good agreement with that observed for $HC(O)OCH_2O_2NO_2$.

3.6. Thermal Stability of $CF_3OC(O)O_2NO_2$.

Acyl peroxy radicals are known to form relatively stable peroxy nitrates.

$$CF_3OC(O)O_2^{\bullet} + NO_2 + M \rightarrow CF_3OC(O)O_2NO_2 + M \quad (4)$$

TABLE 2: Band Centers (in cm^{-1}) of the Measured IR Absorptions for $CF_3OC(O)O_2NO_2$, $CH_3OC(O)O_2NO_2$, $CF_3OCH_2O_2NO_2$, $CH_3OCH_2O_2NO_2$, and $HC(O)OCH_2O_2NO_2$

	band center, cm^{-1}
$CF_3OCH_2O_2NO_2$	793 (NO_2 def), 994, 1073, 1135, 1194, 1232, 1283, 1304 (NO_2 sym str), 1735 (NO_2 asym str)
$CF_3OC(O)O_2NO_2$	791 (NO_2 def), 1007, 1164, 1257, 1298 (NO_2 sym str), 1759 (NO_2 asym str), 1843 and 1875 (CO str)
$CH_3OCH_2O_2NO_2$	794 (NO_2 def), 921, 1099, 1171, 1215, 1297 (NO_2 sym str), 1723 (NO_2 asym str)
$CH_3OC(O)O_2NO_2$	797 (NO_2 def), 928, 1197, 1235, 1304 (NO_2 sym str), 1448, 1748 (NO_2 asym str), 1836 (CO str)
$HC(O)OCH_2O_2NO_2$	793 (NO_2 def), 988, 1112, 1161, 1297 (NO_2 sym str), 1732 (NO_2 asym str), 1772 (CO str)

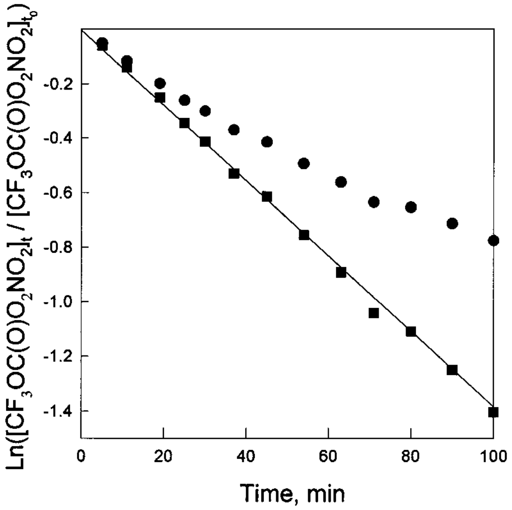

Figure 5. Thermal decomposition of $CF_3OC(O)O_2NO_2$ at 295.8 K. Circles indicate the measured data, and squares indicate the result of correction for regeneration via reaction 4.

The peroxy nitrates decompose via the reverse reaction.

$$CF_3OC(O)O_2NO_2 + M \rightarrow CF_3OC(O)O_2^{\bullet} + NO_2 + M \quad (-4)$$

The decomposition of $CF_3OC(O)O_2NO_2$ was studied in an excess of NO, which removes the $CF_3OC(O)O_2^{\bullet}$ radicals via reaction 3a and thereby precludes the reformation of the peroxy nitrate.

Trifluoromethyl formate was generated in the chamber by UV radiation of gas mixtures of CF_3OCH_3 and Cl_2 in 500 Torr of O_2. When all (>95%) of the CF_3OCH_3 was converted into $CF_3OC(O)H$, NO_2 was added to the reaction mixture and the UV irradiation was resumed which resulted in the formation of $CF_3OC(O)O_2NO_2$. In the absence of added NO, there was no observable (<2%) loss of $CF_3OC(O)O_2NO_2$ on standing in the dark in the chamber for 25 min.

NO was added to the chamber, and the loss of $CF_3OC(O)O_2NO_2$ was monitored at a total pressure of 700 Torr and a temperature of 295.8 ± 0.5 K. The loss was measured relative to the initial concentration of the peroxy nitrate, using its infrared features at 792 and 1006 cm^{-1}. Figure 5 shows the logarithm of the measured peroxy nitrate loss as a function of time (circles). A complication in this experiment is the unavoidable presence of NO_2 in the reaction chamber that leads to regeneration of $CF_3OC(O)O_2NO_2$ via reaction 4. The observed rate of $CF_3OC(O)O_2NO_2$ decay, k_{obs}, is related to the true rate of decay, k_{-4}, by the expression

$$k_{-4} = k_{obs}\left(1 + \frac{k_4[NO_2]}{k_3[NO]}\right) \quad (IV)$$

The concentrations of NO and NO_2 in the chamber were monitored using their characteristic IR absorptions. The rate constant ratio, k_4/k_3, has not been reported, but it seems reasonable to assume that k_4/k_3 will be similar to that measured for the analogous reactions of $CF_3C(O)O_2^{\bullet}$ radicals. Accordingly, we have assumed a value of $k_4/k_3 = 0.64$.[27] The corrected data are shown by squares in Figure 5. A linear regression of the corrected data points gives the rate constant at 295.8 K, $k_{-4} = (2.3 \pm 0.1) \times 10^{-4}$ s^{-1}.

The value of k_{-4} derived here can be compared with those of similar acyl peroxy nitrates. The rates of decomposition of $CH_3C(O)O_2NO_2$ (PAN), $CF_3C(O)O_2NO_2$, and $CH_3OC(O)O_2NO_2$ at 295.8 K are 3.0×10^{-4} s^{-1},[28] 5.3×10^{-5} s^{-1},[29] and 6.1×10^{-4} s^{-1},[24] respectively. This series of data suggests (i) that fluorinated acyl peroxy nitrates are more stable than their nonfluorinated analogs, and (ii) that the presence of the –O– group tends to increase the rate of decomposition.

4. Implications for Atmospheric Chemistry

The kinetics of the reaction of OH radicals with CF_3OCH_3 have been the subject of three studies.[5–7] The early work of Zhang et al.[6] is superseded by that of Orkin et al.[7] and is not considered further. The results reported by Hsu et al.[5] and Orkin et al.[7] are in good agreement and give $k_1 = 1.2 \times 10^{-14}$ cm^3 molecule^{-1} s^{-1} at 298 K. Assuming an atmospheric lifetime for methane of 9 years[30] and a rate constant for the $CH_4 + OH$ reaction of 6.3×10^{-15} cm^3 molecule^{-1} s^{-1} leads to an atmospheric lifetime of CF_3OCH_3 against reaction with OH of ≈4.7 year.

Reaction with OH gives the alkyl radical $CF_3OCH_2^{\bullet}$ which is rapidly converted into the corresponding peroxy radical $CF_3OCH_2O_2^{\bullet}$. As with other alkyl peroxy radicals, the atmospheric fate of $CF_3OCH_2O_2^{\bullet}$ radicals will be reaction with either NO, NO_2, HO_2, or other peroxy radicals. We show here that reaction of $CF_3OCH_2O_2^{\bullet}$ radicals with HO_2 gives $CF_3OC(O)H$ in a yield of 80 ± 11%. Reaction of $CF_3OCH_2O_2^{\bullet}$ radicals with NO_2 gives a thermally unstable peroxy nitrate which will decompose to regenerate the $CF_3OCH_2O_2^{\bullet}$ radicals. Reaction of $CF_3OCH_2O_2^{\bullet}$ radicals with NO produces the alkoxy radical $CF_3OCH_2O^{\bullet}$. It is shown here that the sole fate of the alkoxy radical $CF_3OCH_2O^{\bullet}$ is reaction with O_2 to give the formate, $CF_3OC(O)H$. This is entirely consistent with the behavior of the structurally similar alkoxy radicals, such as $i\text{-}C_4F_9OCH_2O^{\bullet}$,[15] $CH_3OCH_2O^{\bullet}$,[13] and $(CH_3)_3COCH_2O^{\bullet}$ [20] radicals, which are known to exclusively react with O_2 to give formates. Irrespective of whether the oxidation of CF_3OCH_3 occurs in high or low NO_x environments, the formate $CF_3OC(O)H$ is the major primary oxidation product.

It is reported herein that the formate $CF_3OC(O)H$ is rather unreactive toward Cl atoms and is likely to be similarly unreactive toward OH radicals. Organic compounds which react with Cl atoms with rate constants in the range 10^{-14}–10^{-13} cm^3 molecule^{-1} s^{-1} generally react faster with Cl atoms than with OH radicals.[11] Hence, we can use the value of $k_{10} = 9.8 \times 10^{-15}$ cm^3 molecule^{-1} s^{-1} as an upper limit to $k(OH + CF_3OC(O)H)$. Using a 24 h global average OH concentration of 7.5×10^5 cm^{-3}, we derive a lower limit of 3.8 years for the atmospheric lifetime of $CF_3OC(O)H$ with respect to reaction with OH radicals. In view of the polar nature of $CF_3OC(O)H$ it seems likely that the main atmospheric removal mechanism of this compound will be via wet/dry deposition and possibly

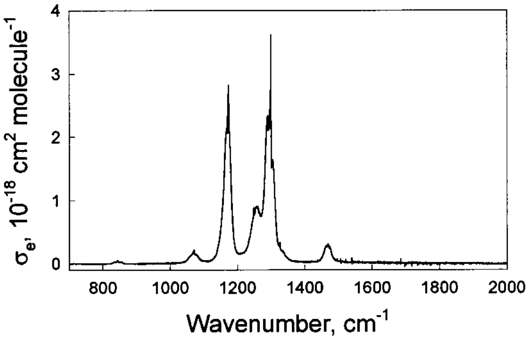

Figure 6. Infrared spectrum of CF_3OCH_3.

photolysis. Unfortunately, there are no available data for the rates of these processes, and hence, it is not possible to provide an estimate of the atmospheric lifetime of $CF_3OC(O)H$ at this time.

The method of Pinnock et al.[31] was used to calculate the instantaneously cloudy-sky radiative forcing of CF_3OCH_3, from the measured absorption cross section. The infrared spectrum of CF_3OCH_3 is shown in Figure 6. The instantaneous radiative forcings of CF_3OCH_3 and CFC-11 were calculated to be 0.19 and 0.26 W/m^2, respectively. The global warming potential (GWP) was estimated using the expression

$$\mathrm{GWP}_t = \frac{\mathrm{IF}_{\mathrm{CF_3OCH_3}}}{\mathrm{IF}_{\mathrm{CFC-11}}} \frac{\tau_{\mathrm{CF_3OCH_3}}}{\tau_{\mathrm{CFC-11}}} \frac{M_{\mathrm{CFC-11}}}{M_{\mathrm{CF_3OCH_3}}} \frac{1 - \exp\left(-\frac{t}{\tau_{\mathrm{CF_3OCH_3}}}\right)}{1 - \exp\left(-\frac{t}{\tau_{\mathrm{CFC-11}}}\right)}$$

where IF, τ, and M are the radiative forcing, lifetime, and molecular weight of the two compounds and t is the time horizon over which the forcing is integrated. Using $\tau_{\mathrm{CF_3OCH_3}} = 4.7$ years and $\tau_{\mathrm{CFC-11}} = 50$ years,[31] we estimate that the GWP of CF_3OCH_3 is ≈ 0.28 for a 20 year horizon and ≈ 0.11 for a 100 year time horizon. The GWP_{100} of CF_3OCH_3 is 5−15 times less than those of typical CFCs, like CFC-11, CFC-12, and CFC-13.

Acknowledgment. We thank Vladimir Orkin (National Institute of Standards and Technology) for supplying the sample of CF_3OCH_3 and Bill Schneider (Ford), Ole John Nielsen (Risø National Laboratory), and Jens Sehested (Haldor Topsø) for helpful discussions.

References and Notes

(1) E-mail: twalling@ford.com.

(2) Molina, M. J.; Rowland, F. S. *Nature* **1974**, *249*, 810.

(3) Farman, J. D.; Gardiner, B. G.; Shanklin, J. D. *Nature* **1985**, *315*, 207.

(4) Product information sheet from 3M Specialty Chemicals Division, 1996.

(5) Hsu, K.-J.; DeMore, W. B. *J. Phys. Chem.* **1995**, *99*, 11141.

(6) Zhang, Z.; Saini, R. D.; Kurylo, M. J.; Huie, R. E. *J. Phys. Chem.* **1992**, *96*, 9301.

(7) Orkin, V. L.; Khamaganov, V. G.; Guschin, A. G.; Huie, R. E.; Kurylo, M. J. Presented at the 13th International Symposium on Gas Kinetics, University College, Dublin, Ireland, 1994.

(8) Wallington, T. J.; Schneider, W. F.; Worsnop, D. R.; Nielsen, O. J.; Sehested, J.; Debruyn, W. J.; Shorter, J. A. *Environ. Sci. Technol.* **1994**, *28*, 320.

(9) Wallington, T. J.; Japar, S. M. *J. Atmos. Chem.* **1989**, *9*, 399.

(10) Vésine, E.; Mellouki, A. *J. Chim. Phys.* **1997**, *94*, 1634.

(11) DeMore, W. B.; Sander, S. P.; Golden, D. M.; Hampson, R. F.; Kurylo, M. J.; Howard, C. J.; Ravishankara, A. R.; Kolb, C. E.; Molina, M. J. *JPL Publ. 97−4*, **1997**.

(12) Wallington, T. J.; Hurley, M. D. *Chem. Phys. Lett.* **1992**, *189*, 437.

(13) Jenkin, M. E.; Hayman, G. D.; Wallington, T. J.; Hurley, M. D.; Ball, J. C.; Nielsen, O. J.; Ellerman, T. *J. Phys. Chem.* **1993**, *97*, 11712.

(14) Wallington, T. J.; Hurley, M. D.; Ball, J. C.; Jenkin, M. E. *Chem. Phys. Lett.* **1993**, *211*, 41.

(15) Wallington, T. J.; Schneider, W. F.; Sehested, J.; Bilde, M.; Nielsen, O. J.; Christensen, L. K.; Molina, M. J.; Molina, L. T.; Wooldridge, P. W. *J. Phys. Chem. A.* **1997**, *101*, 8264.

(16) Ravishankara, A. R.; Turnipseed, A. A.; Jensen, N. R.; Barone, S.; Mills, M.; Howard, C. J.; Solomon, S. *Science* **1994**, *263*, 71.

(17) Mallard, W. G.; Westley, F.; Heron, J. T.; Hampson, R. F. *NIST Chemical Kinetic Database, Version 6.0*; NIST: Washington, DC, 1994.

(18) Wallington, T. J.; Hurley, M. D.; Fracheboud, J.-M.; Orlando, J. J.; Tyndall, G. S.; Sehested, J.; Møgelberg, T. E.; Nielsen, O. J. *J. Phys. Chem.* **1996**, *100*, 18116.

(19) Møgelberg, T. E.; Sehested, J.; Tyndall, G. S.; Orlando, J. J.; Fracheboud, J.-M.; Wallington, T. J. *J. Phys. Chem. A* **1997**, *101*, 2828.

(20) Japar, S. M.; Wallington, T. J.; Richert, J. F. O.; Ball, J. C. *Int. J. Chem. Kinet.* **1990**, *22*, 1257.

(21) Atkinson, R.; Baulch, D. L.; Cox, R. A.; Hampson, R. F.; Kerr, J. A.; Rossi, M. J.; Troe, J. *J. Phys. Chem. Ref. Data* **1997**, *26*, 521.

(22) Wallington, T. J.; Hurley, M. D.; Schneider, W. F.; Sehested, J.; Nielsen, O. J. *Chem. Phys. Lett* **1994**, *218*, 34.

(23) Wallington, T. J.; Hurley, M. D.; Schneider, W. F. *Chem. Phys. Lett.* **1996**, *251*, 164.

(24) Kirchner, F.; Thüner, L. P.; Barnes, I.; Becker, K. H.; Donner, B.; Zabel, F. *Environ. Sci. Technol.* **1997**, *31*, 1801.

(25) Gaffney, J. S.; Fajer, R.; Senum, G. I. *Atmos. Environ.* **1984**, *18*, 215.

(26) Platz, J.; Christensen, L. K.; Sehested, J.; Nielsen, O. J.; Wallington, T. J.; Sauer, C.; Barnes, I.; Becker, K. H.; Vogt, R. *J. Phys. Chem.* **1998**, *102*, 4829.

(27) Zabel, F.; Kirchner, F.; Becker, K. H. *Int. J. Chem. Kinet.* **1994**, *26*, 827.

(28) Sehested, J.; Christensen, L. K.; Møgelberg, T.; Nielsen, O. J.; Wallington, T. J.; Gushin, A.; Orlando, J. J.; Tyndall, G. S. *J. Phys. Chem.* **1998**, *102*, 1779.

(29) Wallington, T. J.; Sehested, J.; Nielsen, O. J. *Chem. Phys. Lett.* **1994**, *226*, 563.

(30) Prinn, R. G.; Weiss, R. F.; Miller, B. R.; Huang, J.; Alyea, F. N.; Cunnold, D. M.; Fraser, P. J.; Hartley, D. E.; Simmonds, P. G. *Science* **1995**, *269*, 187.

(31) Pinnock, S.; Hurley, M. D.; Shine, K. P.; Wallington, T. J.; Smyth, T. J. *J. Geophys. Res.* **1995**, *100*, 23227.